A Self-Calibrating Bipartite Viscosity Sensor for Mitochondria

Zhigang Yang,[†] Yanxia He,[†] Jae-Hong Lee,[†] Nayoung Park,[†] Myungkoo Suh,[⊥] Weon-Sik Chae,[§] Jianfang Cao,[∥] Xiaojun Peng,[∥] Hyosung Jung,[†] Chulhun Kang,*,[‡] and Jong Seung Kim*,[†]

[†]Department of Chemistry, Korea University, Seoul 136-701, Korea

[⊥]Department of Applied Chemistry, Kyung Hee University, Yongin 446-701, Korea

[§]Gangneung Center, Korea Basic Science Institute, Gangneung 210-702, Korea

[‡]The School of East-West Medical Science, Kyung Hee University, Yongin 446-701, Korea

[∥]State Key Laboratory of Fine Chemicals, Dalian University of Technology, Dalian 116024, P. R. China

S *Supporting Information*

ABSTRACT: A self-calibrating bipartite viscosity sensor **1** for cellular mitochondria, composed of coumarin and boron-dipyrromethene (BODIPY) with a rigid phenyl spacer and a mitochondria-targeting unit, was synthesized. The sensor showed a direct linear relationship between the fluorescence intensity ratio of BODIPY to coumarin or the fluorescence lifetime ratio and the media viscosity, which allowed us to determine the average mitochondrial viscosity in living HeLa cells as ca. 62 cP (cp). Upon treatment with an ionophore, monensin, or nystatin, the mitochondrial viscosity was observed to increase to ca. 110 cP.
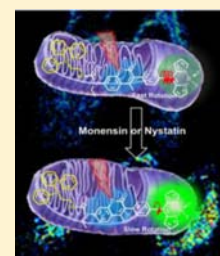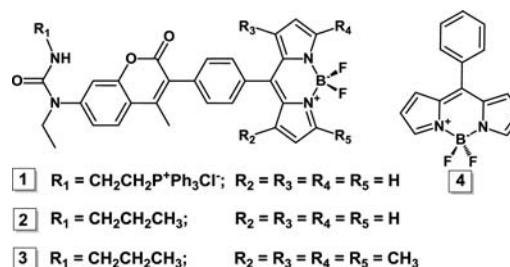
INTRODUCTION

Intracellular viscosity is a critical factor governing the transportation of mass and signals as well as interactions between biomacromolecules. Indeed, it has been demonstrated as a vital contributor or indicator for atherosclerosis,[1] diabetes,[2] Alzheimer's disease,[3] and even cell malignancy,[4] because it affects protein−protein interactions in cellular membranes.[4,5] Furthermore, the viscosity in the mitochondrial matrix is closely related to the respiratory state of the mitochondria via the molecular consequences of mechanically or osmotically induced changes in mitochondrial network organization, which suggests that changes in mitochondrial matrix viscosity may modulate metabolite diffusion and, in turn, mitochondrial metabolism.[1,4,5]

For intracellular viscosity measurement, sensors with dual fluorescent moieties have been introduced, including a Förster resonance energy transfer (FRET) system[6] composed of a flexible linker, energy donor, and energy acceptor. This system offers the advantage that the fluorescence intensity of the viscosity-dependent fluorophore is calibrated to that of the viscosity-independent moiety.[7] However, the relative orientation of the two fluorophores in the system may vary according to media, dye concentration, and other experimental or instrumental factors,[8] which may result in ambiguous conclusions regarding viscosity measurements. Therefore, it would be ideal to design a molecular pair, such as a TBET cassette,[9−22] where the distance between energy donor and acceptor is fixed to minimize uncertainty and to provide "molecular rotors"[6,23−33] that are mainly sensitive to viscosity changes. Moreover, the addition of a mitochondrial guiding unit, which is well demonstrated in the literature,[34] to the mainframe would provide a mitochondrial matrix viscosity sensor with self-calibrating ability.

In this context, we herein describe a self-calibrating bipartite viscosity sensor **1** (Scheme 1) consisting of coumarin and

Scheme 1. Chemical Structures of Targeting Compounds

1	$R_1 = CH_2CH_2P^+Ph_3Cl^-$;	$R_2 = R_3 = R_4 = R_5 = H$
2	$R_1 = CH_2CH_2CH_3$;	$R_2 = R_3 = R_4 = R_5 = H$
3	$R_1 = CH_2CH_2CH_3$;	$R_2 = R_3 = R_4 = R_5 = CH_3$

boron-dipyrromethene (BODIPY) as a fluorescent reporter, with a rigid phenyl spacer and triphenylphosphonium as a mitochondria-targeting unit. The C−C bond between the phenyl spacer and BODIPY can freely rotate to produce fluorescence quenching in a low-viscosity environment, whereas the rotation is restricted to offer fluorescence enhancement in highly viscous media.[6,23−33] Analysis of the fluorescence ratiometry (I_{516}/I_{427}) and fluorescence lifetime (τ_{516}) of sensor **1** can be used to quantify mitochondrial viscosity and also to demonstrate changes in viscosity in the mitochondrial matrix caused by drugs, such as monensin and nystatin.[35,36]

Scheme 2. Synthetic Routes for Compounds 1−4[a]
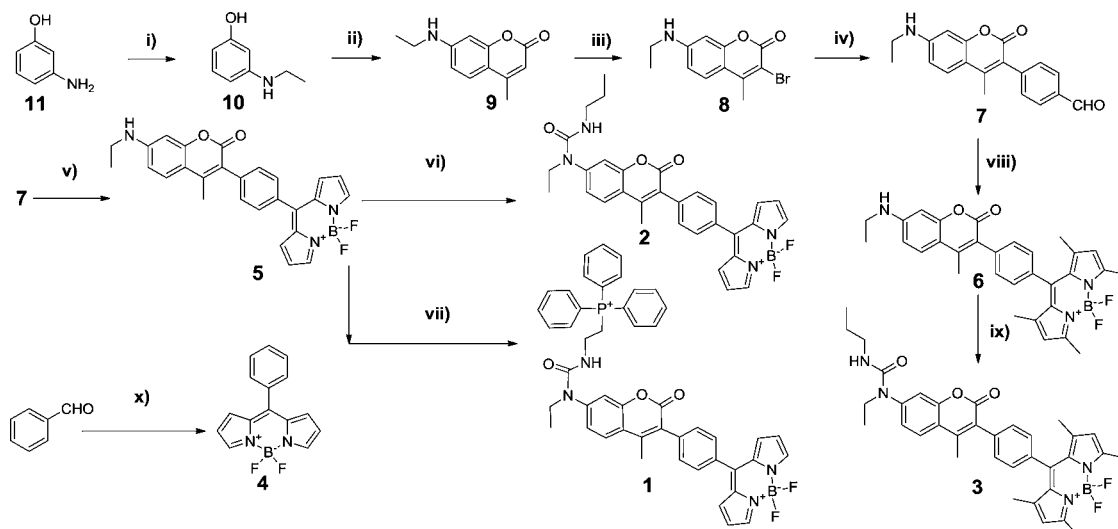
[a](i) ICH$_2$CH$_3$/K$_2$CO$_3$, DMF, 60 °C, 2 h, 75%; (ii) CH$_3$COCH$_2$COOEt/ZnCl$_2$, ethanol, reflux, 12 h, 77%; (iii) NBS, DMF, rt, 41%; (iv) 4-formylphenylboronic acid/Pd(PPh$_3$)$_4$/K$_2$CO$_3$/DME, reflux, 12h, 36%; (v) pyrrole/TFA, DCM, rt, 1 h, then DDQ, DCM, rt, 1 h, then BF$_3$-Et$_2$O, Et$_3$N, DCM, rt, 1 h, 10%; (vi) phosgene/DIPEA, DCM, rt, 1 h, then CH$_3$(CH$_2$)$_2$NH$_2$, DCM, rt, 6 h, 11%; vii) phosgene/DIPEA, DCM, rt, 1 h, then PPh^{3+}(CH$_2$)$_2$NH$_2$Cl$^-$, DCM, rt, 6 h, 10%; (viii) 2,4-dimethylpyrrole/TFA, DCM, rt, 1 h, then DDQ, DCM, rt, 1 h, then BF$_3$-Et$_2$O, Et$_3$N, CH$_2$Cl$_2$, rt, 1 h, 10%; (ix) phosgene/DIPEA, DCM, rt, 1 h, then CH$_3$(CH$_2$)$_2$NH$_2$, DCM, rt, 6 h, 12%; (x) pyrrole/TFA, DCM, rt, 1 h, then DDQ, DCM, rt, 1 h, then BF$_3$-Et$_2$O, Et$_3$N, DCM, rt, 1 h, 10%.

■ RESULTS AND DISCUSSION

To measure mitochondrial viscosity, we synthesized a molecular rotor 1 and the related reference compounds 2−4 (Scheme 2). First, reaction of 3-aminophenol (11) with iodoethane in DMF yielded 10, which further reacted with ethyl acetoacetate in the presence of ZnCl$_2$ to produce the coumarin derivative 9. Subsequently, bromination of 9 yielded compound 8, which underwent a Suzuki coupling reaction using pinacol-4-formylphenylboronate with Pd(PPh$_3$)$_4$ as a catalyst to afford 7. Reaction of 7 with pyrrole and 2,4-dimethylpyrrole resulted in good yields of 5 and 6, respectively. Finally, 7 and 8 reacted with phosgene and the corresponding amines yielded 1−3. Phenyl-BODIPY 4 was also prepared as a reference. All detailed synthetic procedures and their spectral data, including ^{1}H NMR, ^{13}C NMR, and mass analysis data, are described in the Supporting Information.

To characterize the spectral properties of the sensors, we first studied the solvent dependency of 2. Compound 2 reveals two different absorption and emission bands that are mainly contributed by its coumarin and BODIPY moieties (Figure 1A), as determined by theoretical calculation using Gaussian 09 software[37] (Figure S1). In methanol, the emissions of the
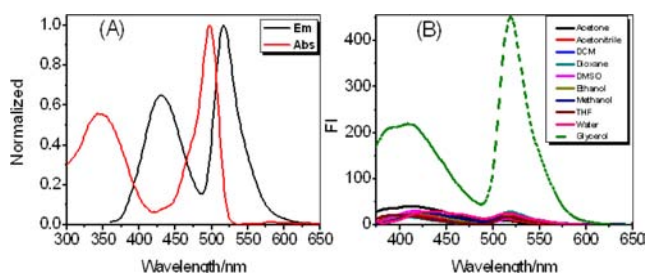
coumarin and BODIPY parts are at 427 and 516 nm, respectively. We found that the emission bands were relatively unaltered even in various solvents but markedly changed in glycerol medium (Figure 1B). Table S1 summarized the fluorescence quantum yields of 2−4 in solvents with various viscosities. The quantum yields of 2 were less than 0.02 in low-viscosity media, regardless of solvent polarity (e.g., in methanol, η = 0.60 cP, ε = 32.63) (Table S1). Only in viscous glycerol (η = 945.35 cP, ε = 42.5), the compound was highly fluorescent and showed a quantum yield of 0.40. Moreover, the quantum yields of 3 containing a tetramethyl moiety were all over 0.3, regardless of the solvent viscosity. These results are attributable to viscosity-dependent rotation of the C−C bond between the BODIPY and the phenyl unit, where the rotation through the C−C bond is restricted in the presence of a highly viscous solvent, such as glycerol, and the excited energy is reserved for emission without nonradiative energy dissipation throughout the rotation. In compound 3, such restriction in the rotational motion is imposed on BODIPY to result in a strong emission, regardless of solvent viscosity. In addition, for animal application, it may be important to note that the coumarin moiety in 2 has a two-photon absorption property with a 30 GM two-photon cross-section (740 nm in 50:50 v/v methanol-glycerol) (Figure S2).

To investigate the relationship between the change in viscosity and the change in fluorescence intensity, fluorescence spectroscopy was performed, and the fluorescence lifetime of the synthesized compounds was measured. As shown in Figure 2, compound 1 showed two emission peaks at 427 and 516 nm, where both emission intensities were found to be enhanced by the solvent viscosity. Relative to the emission of the coumarin moiety at 427 nm (Figure S3), the green emission of BODIPY (516 nm) was more considerably increased with increased solvent viscosity (Figure 2A). We then found a direct linear relationship (R^2 = 0.995, Figure 2B) from a plot of the intensity ratio (I_{516}/I_{427}) vs the solvent viscosity (η). Therefore,

Figure 1. Normalized absorption and fluorescence spectra (A) of 2 in methanol and (B) fluorescence response of 2 (1.0 μM) to different solvents, excited at 330 nm, slit width 3/5.
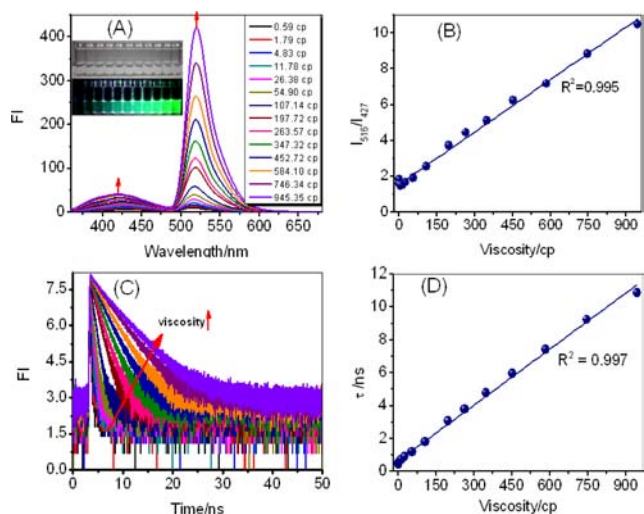
Figure 2. Changes of fluorescent spectra (A) and fluorescence decay (C) of **1** (1.0 μM) with the variation of solution viscosity (methanol-glycerol system). Relationship of the I_{516}/I_{427} ratio (B) and fluorescence lifetime (D) with solution viscosity. Upon excitation at 375 nm, the fluorescence lifetime was measured on a Fluo time 200 single-photon counting equipment. Inset in A, color and fluorescence changes of **1** (1.0 μM) in mixed solvents (methanol-glycerol) with various viscosities under sunlight and a UV lamp (365 nm excitation).

Figure 3. Confocal laser fluorescence microscopic images of HeLa cells treated with **1** and Mito-tracker Red (0.5 μM) or Lyso-Sensor Blue DND-167 (1.0 μM). (A) and (D) Fluorescence imaging of **1** in HeLa cells, collected at 500−600 nm and excited at 720 nm (two-photon excitation). (B) Fluorescent image of Mito-Tracker Green FM (0.5 μM), collected by a 530−570 nm band path filter with excitation at 514 nm. (C) Merged image of A and B. (E) Fluorescent image of Lyso-Sensor Blue DND-167 (1.0 μM), collected by a filter of 370−550 nm upon excitation at 740 nm (two-photon excitation). (F) Merged image of (D) and (E). The scale bars indicate 20 μM.
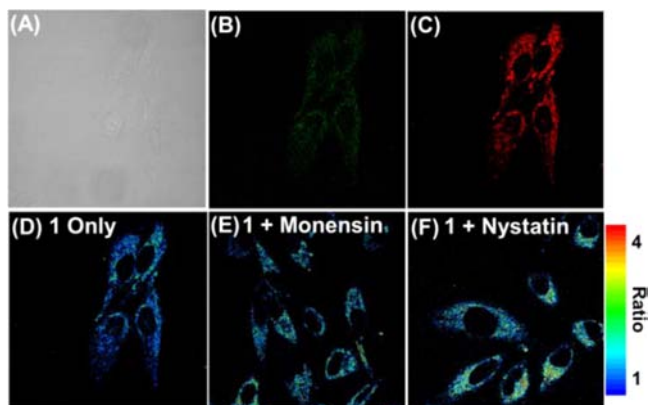
Figure 4. Confocal laser fluorescence imaging (B and C) of **1** (2.0 μM) in HeLa cells and ratiometric image (D−F) obtained by ImagePro Plus software and imaging of fluorescence duration. (A) Bright-field image of HeLa cells. (B) Blue-channel fluorescence images detected at 370−470 nm upon excitation at 720 nm. (C) Green-channel fluorescence images detected at 500−600 nm upon excitation at 720 nm. (D) Ratiometric image of **1** in HeLa cells obtained by dividing image (B) by image (A) in ImagePro Plus software. (E) and (F) are ratiometric images of **1** in HeLa cells upon treatment with monensin and nystatin, respectively.

compound **1** could be employed to ratiometrically detect viscosity in various media, including biological systems. However, we found that the ratio rarely depends on the solvent polarity (Figure S4). In addition, the lifetime (τ_f) of **1** at 516 nm increased gradually as the viscosity increased (Figure 2C); in particular, a linear relationship was observed between fluorescence duration (τ_f) and solvent viscosity (η) ($R^2 = 0.997$) (Figure 2D). Similar relationships in the case of refs 2 and 4 (Figures S6 and S7) were also obtained in water-glycerol systems, as shown in Figure S5. For **3**, which bears sterically hindered tetramethyl-substituted BODIPY, the intensity ratio and fluorescence lifetime revealed were relatively unchanged, as we expected (Figure S8).

To utilize rotor **1** as a mitochondrial viscosity sensor, its intracellular location has to be characterized prior to viscosity measurement. Colocalization results obtained using a confocal laser microscope with mitochondrial and lysosomal markers are shown in panels (A−C) and (D−F) in Figure 3, respectively. The yellow parts in panels (C) and (F) represent the colocalization of **1** with Mito-Tracker and Lyso-Sensor, respectively, and indicate that **1** is mainly located in the mitochondria (C). In parallel experiments, probes **2** and **3** without the mitochondrial targeting unit fail to show intense yellow images with Mito-Tracker Green FM (Figures S9 and S10), which confirms that the mitochondrial preference of rotor **1** originates from its triphenylphosphonium moiety.

To validate sensor **1** for mitochondrial viscosity imaging, confocal laser fluorescence images of HeLa cells were acquired in the presence of two different ionophores (monensin and nystatin). Monensin and nystatin are well-known to induce mitochondrial malfunction caused by structural changes or swelling of mitochondria.[35,36] Cell images based on the coumarin and BODIPY emissions of **1** are shown in Figure 4B,C. Panel (D) is a ratiometric image based on I_{516}/I_{427} obtained from (B) and (C) and pseudocolored using ImagePro Plus software. The average fluorescence ratio was ca. 2.17.
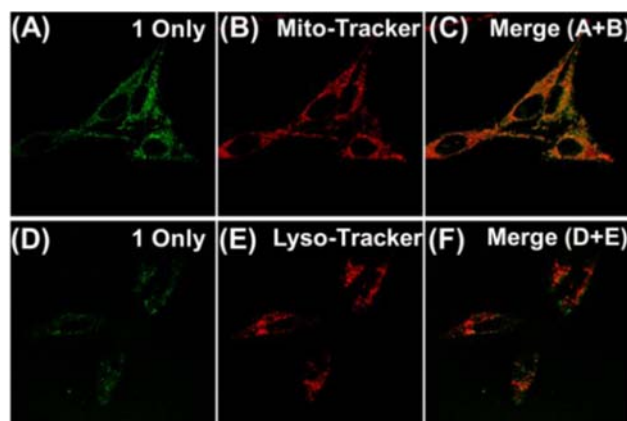
From the linear relationship between the ratio and the viscosity established in Figure 2B, the average viscosity of mitochondria in HeLa cells was estimated as ca. 62.8 cP. Upon treatment with monensin and nystatin, which may cause mitochondrial swelling through interruption of the ionic balance,[38,39] the images corresponding to the ratiometric image in panel (D) revealed apparently enhanced ratios (Figures 5E and F and S11−S14). The I_{516}/I_{427} values were 2.44 ± 0.50 and 2.62 ± 0.48, which were equivalent to 90.5 and 109 cP, upon treatment with monensin and nystatin, respectively. The increased viscosity in ionophore-treated mitochondria agrees with previous findings and indicates that these ionophores can induce ultrastructural changes[35] or swelling[38,39] of mitochon-
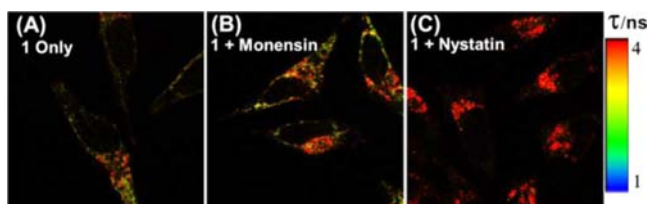
Figure 5. Fluorescence lifetime images of **1** (2.0 μM) in HeLa cells. (A) Control and (B) **1** incubated with HeLa cells, then incubated with monensin. (C) **1** incubated with HeLa cells, then incubated with nystatin. Equipment: inverted-type scanning confocal microscope (MicroTime-200, Picoquant, Germany) with a 60× objective (NA = 1.2) and a single-mode pulsed diode laser (375 nm with a pulse width of ~240 ps in full width at half-maximum and an average power of ~5 μW). The excitation and detection wavelengths, 375 and 516 nm, respectively.

dria or large-scale alteration of mitochondrial metabolism.[36] Even in the absence of a detailed description of the underlying mechanism, these data provide sufficient evidence for the validity of sensor **1** as a mitochondrial viscosity sensor in the context of metabolic changes in mitochondria.

To justify the results of the ratiometric measurement of mitochondrial viscosity shown in Figure 4, a fluorescence lifetime imaging (FLIM) experiment was also conducted, as shown in Figure 5A. The mitochondrial fluorescence lifetime of sensor **1** in HeLa cells was measured as ca. 1.4 ns, which indicates a viscosity of ca. 67.5 cP according to the linear relationship shown in Figure 2D. Furthermore, upon the treatment with monensin and nystatin, similar enhancement of the fluorescence lifetime of **1** in mitochondria was observed (B and C). The fluorescence lifetime was ca. 1.55 (B, monensin) and 1.90 ns (C, nystatin), which corresponds to viscosity values of ca. 80.8 (B) and 112 cP (C), respectively, which the results can be comparable to the reported mitochondrial viscosity (54 ± 9 cP in bullfrog myocardium cells).[40] This confirms again that sensor **1** can measure the mitochondrial viscosity responsible for cell apoptosis in living cells by two different methods, i.e., fluorescence ratiometry or FLIM, which has not been previously reported, to the best of our knowledge.

Therefore, the bipartite viscosity sensor **1** is capable of sensing mitochondrial viscosity by fluorescence ratiometry imaging as well as by FLIM within high accuracy and reliability. Scheme 3 summarizes sensing mechanism of rotor **1** toward mitochondrial viscosity in Hela cells with respect to fluorescence ratiometry imaging and FLIM. Sensor **1** shows

Scheme 3. Proposed Mechanism of Rotor 1 Sensing Mitochondrial Viscosity by Fluorescence Ratiometry Imaging and FLIM
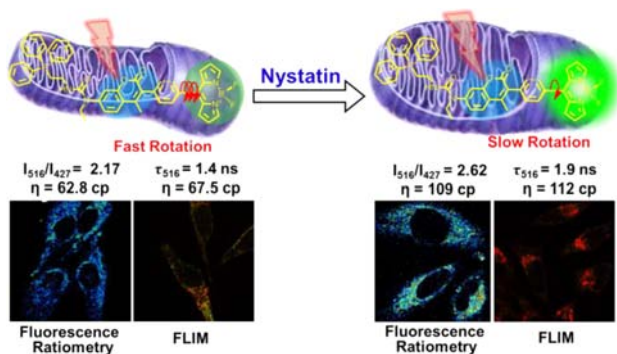
weak emissions in both fluorophores where the BODIPY emission is quenched due to the fast rotation of C−C bond between the phenyl and BODIPY units. Upon treatment of nystatin or monensin, the mitochondria undergo ultrastructural changes or swelling to induce increase in its viscosity, which slows down the C−C bond rotation to markedly enhanced fluorescence from the BODIPY.

CONCLUSIONS

In conclusion, a novel molecular rotor having a triphenylphosphonium and a coumarin-BODIPY dyad with a rigid phenyl spacer has been developed. Both fluorescence ratio values (I_{516}/I_{427}) and fluorescence lifetime (τ_{516}) of rotor **1** are in a good linear relationship with media viscosity. Thereby, the sensor **1** can quantify the mitochodrial viscosity by fluorescence ratiometry and by FLIM with excellent self-calibrtating ability. Furthermore, the rotor **1** also can measure the viscosity changes upon mitochondrial apoptosis induced by treatment of monensin and nystatin. It is therefore believed that the molecular rotor-based bipartite sensor **1** provides a promising strategy in inspecting mitochondrial viscosity and in diagnosis of certain mitochondria related diseases.

ASSOCIATED CONTENT

Ⓢ Supporting Information
Experimental details; synthesis and characteristic data (^{1}H NMR, ^{13}C NMR, mass spectra); fluorescence spectra and fluorescence lifetime measuring; CLSM and FLIM images. This material is available free of charge via the Internet at http://pubs.acs.org.

AUTHOR INFORMATION

Corresponding Author
jongskim@korea.ac.kr; kangch@khu.ac.kr
Notes
The authors declare no competing financial interest.

ACKNOWLEDGMENTS

REFERENCES

(1) Deliconstantinos, G.; Villiotou, V.; Stavrides, J. C. *Biochem. Pharmacol.* **1995**, *49*, 1589−1600.
(2) Nadiv, O.; Shinitzky, M.; Manu, H.; Hecht, D.; Roberts, C. T., Jr.; Leroith, D.; Zick, Y. *Biochem. J.* **1994**, *298*, 443−450.
(3) Zubenko, G. S.; Kopp, U.; Seto, T.; Firestone, L. L. *Psychopharmacology (Berlin)* **1999**, *145*, 175−180.
(4) Shinitzky, M. In: *Physiology of membrane fluidity*; Shinitzky, M., Ed.; CRC Press: Boca Raton, FL, 1984; pp 1−51.
(5) Singer, S. J.; Nicolson, G. L. *Science* **1972**, *175*, 720−731.
(6) Haidekker, M. A.; Brady, T. P.; Lichlyter, D.; Theodorakis, E. A. *J. Am. Chem. Soc.* **2006**, *128*, 398−399.
(7) Luby-Phelps, K.; Mujumdar, S.; Mujumdar, R. B.; Ernst, L. A.; Galbraith, W.; Waggoner, A. S. *Biophys. J.* **1993**, *65*, 236−242.
(8) Fischer, D.; Theodorakis, E. A.; Haidekker, M. A. *Nat. Protoc.* **2007**, *2*, 227−236.
(9) Bozdemir, O. A.; Cakmak, Y.; Sozmen, F.; Ozdemir, T.; Siemiarczuk, A.; Akkaya, E. U. *Chem.—Eur. J.* **2010**, *16*, 6346−6351.
(10) Jiao, G.-S.; Thoresen, L. H.; Burgess, K. *J. Am. Chem. Soc.* **2003**, *125*, 14668−14669.

9184

dx.doi.org/10.1021/ja403851p | *J. Am. Chem. Soc.* 2013, 135, 9181−9185

(11) Han, J.; Jose, J.; Mei, E.; Burgess, K. *Angew. Chem., Int. Ed.* **2007**, *46*, 1684−1687.

(12) Ueno, Y.; Jose, J.; Loudet, A.; Pérez-Bolívar, C.; Anzenbacher, P., Jr.; Burgess, K. *J. Am. Chem. Soc.* **2011**, *133*, 51−55.

(13) Lin, W.; Yuan, L.; Cao, Z.; Feng, Y.; Song, J. *Angew. Chem., Int. Ed.* **2010**, *49*, 375−379.

(14) Jiao, G.-S.; Loudet, A.; Lee, H. B.; Kalinin, S.; Johansson, L. B.-A.; Burgess, K. *Tetrahedron* **2003**, *59*, 3109−3116.

(15) Quade, D. T. M.; Pullen, A. E.; Swager, T. M. *Chem. Rev.* **2000**, *100*, 2537−2574.

(16) Tour, J. M. *Chem. Rev.* **1996**, *96*, 537−554.

(17) Holten, D.; Bocian, D.; Lindsey, J. S. *Acc. Chem. Res.* **2002**, *35*, 57−69.

(18) Kumar, M.; Kumar, N.; Bhalla, V.; Singh, H.; Sharma, P. R.; Kaur, T. *Org. Lett.* **2011**, *13*, 1422−1425.

(19) Bandichhor, R.; Petrescu, A. D.; Vespa, A.; Kier, A. B.; Schroeder, F.; Burgess, K. *J. Am. Chem. Soc.* **2006**, *128*, 10688−10689.

(20) Coskun, A.; Akkaya, E. U. *J. Am. Chem. Soc.* **2005**, *127*, 10464−10465.

(21) Coskun, A.; Akkaya, E. U. *J. Am. Chem. Soc.* **2006**, *128*, 14474−14475.

(22) Diring, S.; Puntoriero, F.; Nastasi, F.; Campagna, S.; Ziessel, R. *J. Am. Chem. Soc.* **2009**, *131*, 6108−6110.

(23) Haidekker, M. A.; Theodorakis, E. A. *Org. Biomol. Chem.* **2007**, *5*, 1669−1678.

(24) Levitt, J. A.; Chung, P.-H.; Kuimova, M. K.; Yahioglu, G.; Wang, Y.; Qu, J.; Suhling, K. *Chem. Phys. Chem.* **2011**, *12*, 662−672.

(25) Kuimova, M. K. *Phys. Chem. Chem. Phys.* **2012**, *14*, 12671−12686.

(26) Zhou, F.; Shao, J.; Yang, Y.; Zhao, J.; Guo, H.; Li, X.; Ji, S.; Zhang, Z. *Eur. J. Org. Chem.* **2011**, *25*, 4773−4787.

(27) Sutharsan, J.; Lichlyter, D.; Wright, N. E.; Dakanali, M.; Haidekker, M. A.; Theodorakis, E. A. *Tetrahedron* **2010**, *66*, 2582−2588.

(28) Liu, F.; Wu, T.; Cao, J.; Cui, S.; Yang, Z.; Qiang, X.; Sun, S.; Song, F.; Fan, J.; Wang, J.; Peng, X. *Chem.—Eur. J.* **2013**, *19*, 1548−1553.

(29) Peng, X.; Yang, Z.; Wang, J.; Fan, J.; He, Y.; Song, F.; Wang, B.; Sun, S.; Qu, J.; Qi, J.; Yan, M. *J. Am. Chem. Soc.* **2011**, *133*, 6626−6635.

(30) Kuimova, M. K.; Botchway, S. W.; Parker, A. W.; Balaz, M.; Collins, H. A.; Anderson, H. L.; Suhling, K.; Ogilby, P. R. *Nat. Chem.* **2009**, *1*, 69−73.

(31) Kuimova, M. K.; Yahioglu, G.; Levitt, J. A.; Suhling, K. *J. Am. Chem. Soc.* **2008**, *130*, 6672−6673.

(32) Levitt, J. A.; Kuimova, M. K.; Yahioglu, G.; Chung, P.-H.; Suhling, K.; Phillips, D. *J. Phys. Chem. C* **2009**, *113*, 11634−11642.

(33) Wang, L.; Xiao, Y.; Tian, W.; Deng, L. *J. Am. Chem. Soc.* **2013**, *135*, 2903−2906.

(34) Lee, M. H.; Han, J. H.; Lee, J.-H.; Choi, H. G.; Kang, C.; Kim, J. S. *J. Am. Chem. Soc.* **2012**, *134*, 17317−17319.

(35) Souza, A. C.; Machado, F. S.; Celes, M., R; Faria, G.; Rocha, L., B.; Silva, J. S.; Rossi, M. A. *J. Vet. Med., A* **2005**, *52*, 230−237.

(36) Soltoff, S. P.; Mandel, L. J. *J. Membr. Biol.* **1986**, *94*, 153−161.

(37) Frisch, M. J.; Trucks, G. W.; Schlegel, H. B.; Scuseria, G. E.; Robb, M. A.; Cheeseman, J. R.; Scalmani, G.; Barone, V.; Mennucci, B.; Petersson, G. A.; Nakatsuji, H.; Caricato, M.; Li, X.; Hratchian, H. P.; Izmaylov, A. F.; Bloino, J.; Zheng, G.; Sonnenberg, J. L.; Hada, M.; Ehara, M.; Toyota, K.; Fukuda, R.; Hasegawa, J.; Ishida, M.; Nakajima, T.; Honda, Y.; Kitao, O.; Nakai, H.; Vreven, T.; Montgomery, J. A., Jr.; Peralta, J. E.; Ogliaro, F.; Bearpark, M.; Heyd, J. J.; Brothers, E.; Kudin, K. N.; Staroverov, V. N.; Kobayashi, R.; Normand, J.; Raghavachari, K.; Rendell, A.; Burant, J. C.; Iyengar, S. S.; Tomasi, J.; Cossi, M.; Rega, N. J.; Millam, M.; Klene, M.; Knox, J. E.; Cross, J. B.; Bakken, V.; Adamo, C.; Jaramillo, J.; Gomperts, R.; Stratmann, R. E.; Yazyev, O.; Austin, A. J.; Cammi, R.; Pomelli, C.; Ochterski, J. W.; Martin, R. L.; Morokuma, K. V.; Zakrzewski, G.; Voth, G. A.; Salvador, P.; Dannenberg, J. J.; Dapprich, S.; Daniels, A. D.; Farkas, O.; Foresman, J. B.; Ortiz, J. V.; Cioslowski, J.; Fox, D. J. *Gaussian 09*, revision A. 02; Gaussian, Inc.: Wallingford, CT, 2009.

(38) Hansson, M. J.; Morota, S.; Teilum, M.; Mattiasson, G.; Uchino, H.; Elmér, E. *J. Biol. Chem.* **2010**, *285*, 741−750.

(39) Hurnák, O.; Zachar, J. *Gen. Physiol. Biophys.* **1995**, *14*, 359−366.

(40) Koyama, T.; Zhu, M.-Y.; Araiso, T.; Kinjo, M.; Kitagawa, H.; Sugimura, M. *Jpn. J. Physiol.* **1990**, *40*, 65−78.